

Document downloaded from:

<http://hdl.handle.net/10251/189675>

This paper must be cited as:

Dare, EO.; Vendrell-Criado, V.; Jiménez Molero, MC.; Pérez-Ruiz, R.; Díaz Díaz, D. (2021). Highly efficient latent fingerprint detection by eight-dansyl-functionalized octasilsesquioxane nanohybrids. *Dyes and Pigments*. 184:1-7. <https://doi.org/10.1016/j.dyepig.2020.108841>



The final publication is available at

<https://doi.org/10.1016/j.dyepig.2020.108841>

Copyright Elsevier

Additional Information

1 **Highly Efficient Latent Fingerprint Detection by Eight-Dansyl-Functionalized** 2 **Octasilsesquioxane Nanohybrids**

3 Enock O. Dare,^{†*} Victoria Vendrell-Criado,[‡] M. Consuelo Jiménez,[‡] Raúl Pérez-Ruiz[‡] and David
4 Díaz Díaz^{†|†*}

5 [†]Institute of Organic Chemistry, University of Regensburg Universitätsstr. 31, 93040, Regensburg,
6 Germany.

7 [‡]Departamento de Química, Universitat Politècnica de València, Camino de Vera s/n, 46022,
8 Valencia, Spain.

9 [|]Departamento de Química Orgánica, Universidad de La Laguna Avda. Astrofísico Francisco
10 Sánchez, 38206, La Laguna, Tenerife, Spain.

11 ^{††}Instituto Universitario de Bio-Orgánica Antonio González, Universidad de La Laguna, Avda.
12 Astrofísico Francisco Sánchez 2, 38206, La Laguna, Tenerife, Spain.

14 **Abstract**

15 The largely demand in security issues makes necessary the development of novel materials with
16 outstanding properties to improve the current detection techniques. In this context, latent fingerprint
17 (LF) by fluorescent labeled materials (FLM) is one of the most attractive personnel identification
18 methodology. Here, two FLM based on polyhedral oligomeric silsesquioxane (POSS) nanohybrids
19 labeled with dansyl chromophores have been synthesized and fully characterized. Their
20 photophysical properties have confirmed that these materials clearly possess the prime qualifications
21 as suitable LF sensing platforms. In fact, they adequately detect LFs on glassy surface in excellence
22 legibility.

23 **Keywords**

24 fingerprint detection • silsesquioxanes • dansyl • click chemistry • photostability

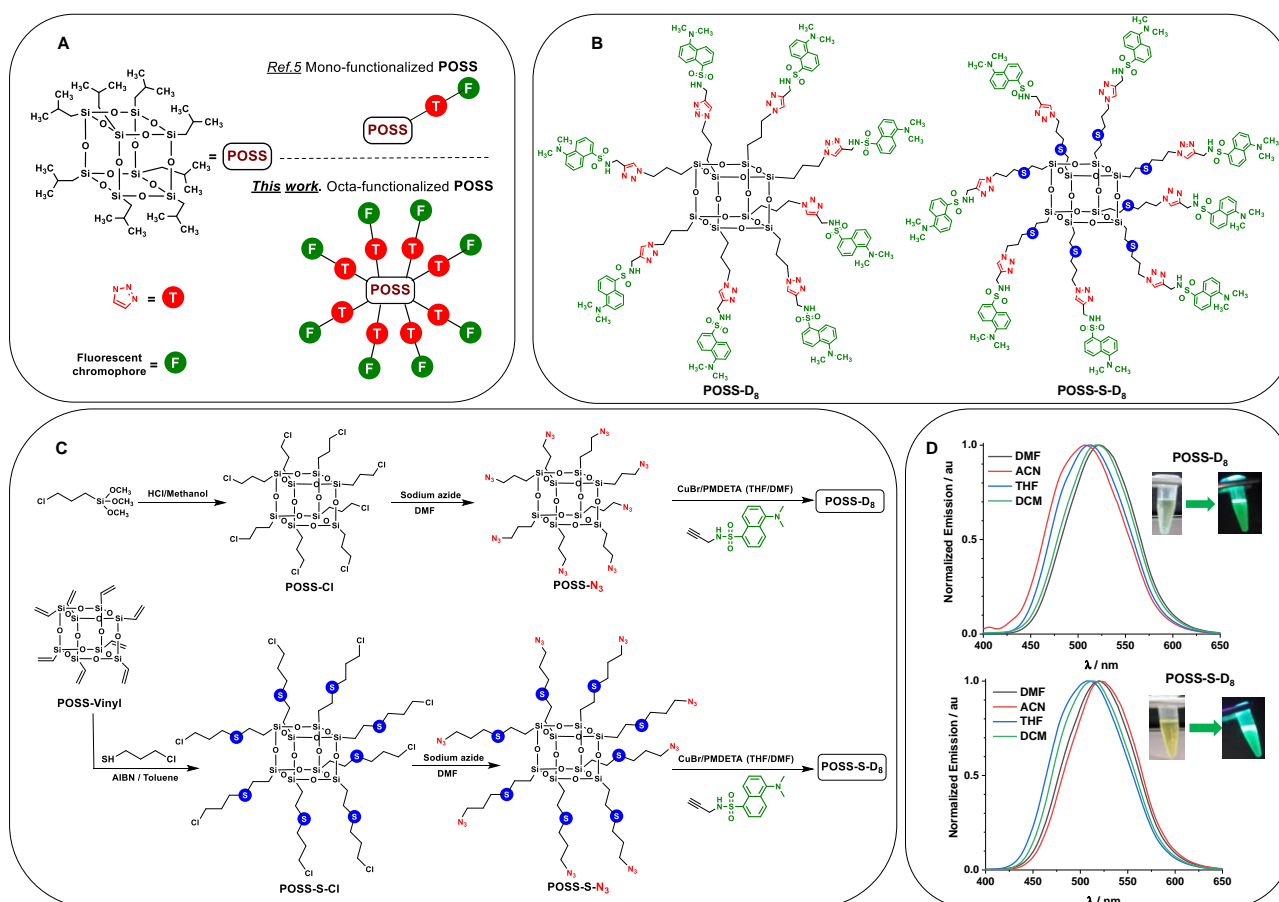
25

26 **1. Introduction**

27 Fluorescent labeled materials (FLMs) are already applying to forensic science such as encoding
28 information for anti-counterfeiting,¹ encryption of confidential data² or latent fingerprint (LF).³ The
29 latter appears to be the best option for personal identification due to their uniqueness and complexity
30 of ridge patterns.⁴ Despite the fact that nanoparticles are found to be a potential tool for LF detection,⁵
31 development of novel systems is still required in order to finally take them into account for routine
32 use. Thus, validate nanoparticles should fulfill three desirable properties at the same time: i) particles
33 with nanometric range (up to 100 nm), ii) to be facilely functionalized onto the surface (to permit the
34 selective targeting of fingermark components) and, iii) to have optical properties that facilitate
35 fingermark visualization post development. In this context, some nanohybrids have appeared to suit
36 these characteristics and can be found in the literature.^{6,7} For instance, Chen and co-workers⁶
37 developed a nanohybrid which exhibited traffic light-type fluorescence color change when exposed
38 to TNT. Thus, red-emitting Cu-doped ZnCdS (Cu-ZnCdS) quantum dots were embedded into silica
39 nanoparticles and the green-emitting ZnCdS quantum dots were anchored onto the surface of the
40 silica nanoparticles and further functionalized with polyallylamine (PAA). Due to this proper
41 structural design, the nanohybrid was capable of both fingerprint staining and drug/explosive
42 visualization. Cui and coworkers⁷ synthesized fluorescent carbon and silica nanohybrids in one
43 simple step which resulted in effective FLMs for the image of LFs on a variety of surfaces including
44 i.e. single background color materials (marbles, transparent tape, white ceramic tiles, black plastic
45 pages, stainless steel sheets, and painted wood) and multicolored surfaces (drink bottle foils and fresh
46 fruits); in this particular case a comparative study with benchmark techniques was however missed.
47 Very recently, we have explored the feasibility of a rigid 3D hetero-structural material based on
48 polyhedral oligomeric silsesquioxane (**POSS**) mono-doped with different chromophores for LFs
49 detection (Figure 1A).⁸⁸ We demonstrated that these cubic octameric frameworks (T8) with an
50 adequate cage size (0.5-0.7 nm), exhibited high stability, excellent biocompatibility in biological

51 environment and effectiveness for LF detection. From a mechanistic point of view, recent studies
52 have shown that hydrophobicity is a major yardstick to fingerprinting development mechanism.^{9,10} In
53 this line, the Si–O–Si skeleton clearly provided hydrophobic properties. In addition, labelling with a
54 dansyl fluorophore was carefully chosen considering not only its photophysical properties (very large
55 Stoke's shift and environment-sensibly) but also hydrophobicity of the 3D nanohybrid remained
56 unaltered. The mechanism of detection implied hydrogen-bonding with the residual amino acids in
57 the fingerprints. In view of the necessity of progressing in the forensic science area and the non-stop
58 evolution on constructing new materials for LF application, we have made a step forward into these
59 promising 3D materials which are barely known. The strategy is now based on anchoring to the Si–
60 O–Si skeleton with eight fluorescent chromophores in order to provide it with unprecedented
61 characteristics in terms of photophysical properties, photostability and great effectiveness on LF
62 detection, pointing to favor hydrogen-bonding interactions (Figure 1A).

63 In this study, two novel eight-dansyl-functionalized POSS nanohybrids have been successfully
64 synthesized (**POSS-D8** and **POSS-S-D8**) following a three-step procedure (Figure 1B). Both
65 nanohybrids fulfil the three prime requisites: i) they fall less than 100 nm, ii) they can be easily
66 functionalized by simple synthetic routes and, iii) they present excellent optical properties for a
67 successful real LF detection.



68

69 **Figure 1.** A) Schematic illustration of the mono- (see ref. 8) and octa-functionalization (this work)
 70 of 3D POSS. B) Chemical structures of octakis(N-dansyl-((1-propyl-1H-1,2,3-triazol-4-
 71 yl)methyl))octasilsequioxane (**POSS-D₈**) and its analogue with thioether bridges (**POSS-S-D₈**). C)
 72 Synthetic routes for **POSS-D₈** and **POSS-S-D₈**. D) Normalized emission spectra ($\lambda_{\text{exc}} = 340$ nm) of
 73 **POSS-D₈** (top) and **POSS-S-D₈** (bottom) in different solvents (DMF = dimethylformamide; ACN =
 74 acetonitrile; THF = tetrahydrofuran; DCM = dichloromethane) under aerobic conditions.
 75 Concentrations were fixed at [**POSS-D₈**] = 0.004 mM and [**POSS-S-D₈**] = 0.04 mM. Insets:
 76 Photographs of both nano hybrids in solution before and after light exposure.

77

78 2. Experimental Section

79 Materials

80 ¹H NMR spectra were recorded on a Bruker Avance 300 or 400 MHz spectrometer in CDCl₃ or
 81 DMSO-d₆. The residual undeuterated solvent signal was used as reference, relative to the

82 tetramethylsilane signal. ^{13}C NMR were recorded on a Bruker Avance 300 or 400 MHz (respective
83 resonance frequency: 75 and 101 MHz) under broadband ^1H decoupling in CDCl_3 or DMSO-d^6 . ^{29}Si
84 NMR were recorded in the same vein. The residual undeuterated solvent signal was used as reference,
85 relative to the tetramethylsilane signal. ^1H NMR and ^{13}C NMR data were reported as follows:
86 Chemical shifts were reported in the δ scale relative to residual CDCl_3 (7.26 ppm) for ^1H NMR and
87 to the central line of CDCl_3 (77.16 ppm) for ^{13}C NMR. FT-IR spectra were obtained with an Agilent
88 Technologies Cary 630 FT-IR spectrometer equipped with Golden Gate Diamond ATR (attenuated
89 total reflection. All reactions were monitored by thin-layer chromatography using Merck silica gel
90 plates 60 F254; visualization was accomplished with short-wavelength UV light (254 nm) and/or
91 staining with appropriate stains (anisaldehyde, orthophosphomolybdic acid). Standard flash
92 chromatography was performed using Macherey-Nagel silica gel of a particle size 40–63 μm . 3-
93 chloropropyltrimethoxysilane, trichlorovinylsilane, amberlite-R120, 3-chloro-1-propanethiol and
94 *N,N,N',N'',N''*-pentamethyldiethylenetriamine (PMDETA) were purchased from Sigma-Aldrich. All
95 other commercially available reagents and solvents were used without further purification.

96 *Synthesis and characterization of compounds*

97 Synthesis of alkynyl dansyl derivative: 5-(dimethylamino)-*N*-(2-propynyl)-1-
98 naphthalenesulfonamide (*N*-dansyl propynyl, **D**) was prepared according to previous procedure.¹¹ ^1H
99 and ^{13}C NMR spectral data for **D** were found to be similar to those found in literature.

100 Synthesis of octakis(3-chloropropyl)octasilsesquioxane (**POSS-Cl**):¹² A solution of 150 mL of dry
101 methanol and 5 mL of concentrated hydrochloric acid was placed in a two-necked, round-bottomed
102 flask equipped with a condenser, an addition funnel, and a magnetic stir bar. To this solution was
103 added dropwise a portion of (3-chloropropyl)trimethoxysilane (15 g, 0.075 mol) through the addition
104 funnel over a period of 10 min with vigorous stirring. The stirring was continued for 2 h until the
105 solution had cooled to room temperature. The reaction mixture was kept at room temperature for
106 another 48 h without stirring. After 2 days, di-*n*-butyltin dilaurate (0.15 g, 0.24 mmol), as a

107 condensation catalyst, was added with stirring. The reaction mixture was maintained at room
108 temperature for 2 days until a white crystalline precipitate appeared. The solution was filtered, and
109 the crystals were collected, washed several times with methanol, and dried under vacuum.

110 ^1H NMR (CDCl_3 , 298 K, 300 MHz; ppm): 0.78 (t, 16H, SiCH_2); 1.84 (q, 16H, CH_2); 3.53 (t, 16H,
111 CH_2Cl). ^{13}C NMR (CDCl_3 , 298 K, 75.5 MHz; ppm): 9.9 (SiCH_2 -); 26.4 ($-\text{CH}_2$ -); 47.1 ($-\text{CH}_2\text{Cl}$). ^{29}Si
112 NMR (CDCl_3 , 298 K, 59.6 MHz; ppm): -67.28.

113 Synthesis of octakis(3-azidopropyl)octasilsesquioxane (**POSS-N₃**):¹³**POSS-Cl** (0.935 mmol, 0.98 g)
114 and NaN_3 (2.13 g) were added to a flask equipped with a magnetic stirrer along with 17 mL of
115 anhydrous *N,N*-dimethylformamide (DMF). The reaction was carried out at 120 °C for 48 h. After
116 completion of the reaction, distilled water was added, and the mixture was extracted with CH_2Cl_2 .
117 Organic layers were dried over anhydrous sodium carbonate, filtered, and concentrated under reduced
118 pressure to obtain the desired product as a yellow viscose liquid.

119 ^1H NMR (CDCl_3 , 500 MHz) δ (ppm): 0.71-0.74 (t, 16H, SiCH_2), 1.66-1.73 (q, 16H, CH_2), 3.25-3.28
120 (t, 16H, CH_2N_3). ^{13}C NMR (CDCl_3 , 125 MHz) δ (ppm): 8.95 (SiCH_2 -), 22.42 ($-\text{CH}_2$), 53.36 ($-\text{CH}_2\text{N}_3$).
121 ^{29}Si NMR (CDCl_3 , 99 MHz) δ (ppm) -67.04.

122 Synthesis of octakis(3-dansylpropyl)octasilsesquioxane (**POSS-D₈**): Under nitrogen atmosphere, to
123 a 10 mL DMF/THF (1:1) solution of **POSS-N₃** (0.1 g, 9.2×10^{-5} mol) was added *N*-dansyl propynyl,
124 **D** (0.24 g, 8.3×10^{-4}). CuBr (50% mol equivalent) and PMDETA (50% mol equivalent) were
125 successively added. The reaction mixture was stirred at RT overnight. 0.02 M EDTA was added and
126 extracted with DCM. Organic phase was further washed with deionized water and Na_2SO_4 added.
127 After filtration and concentration in a rotary evaporator, further purification was achieved in a column
128 chromatography (Hexane: Ethyl acetate, 30%) to afford the desired product as a light yellow solid
129 (0.078 g, yield 78%).

130 ^1H NMR (300 MHz, CDCl_3) δ (ppm): 0.61 (t, 16H, $-\text{SiCH}_2$ -), 1.81 (m, 16H, $\text{Si-CH}_2\text{CH}_2$ -), 2.8 (s,
131 48H, $-\text{N}(\text{CH}_3)_2$), 4.24 (overlapped 16H, $-\text{CH}_2\text{N-}$), 4.25 (overlapped 16H, triazole- $\text{CH}_2\text{NH-}$), 7.15 (s,

132 8H, -CH₂NH-) 7.7 (s, 8H, in 1,2,3-triazole), 7.3-7.5, 8.25-8.3, 8.5 (all d, 6H, CH in dansyl aromatic);
133 ¹³C NMR (125 MHz, CDCl₃) δ (ppm): 102.5, 107, 116, 118, 123, 128, 131. ²⁹Si NMR (59.6 MHz,
134 CDCl₃) δ (ppm): -67.93 (Si-O-Si); FT-IR (cm⁻¹): ν(CH) 2932.6; (CN) 1646; (NCO) 1644.7 ν(C=C-
135 Ar) 1741.9; ν(Si-O-Si) 1161-1020; MS (API-ESI) m/z: 3397.40 [M+H]⁺. Elemental analysis:
136 calculated for C₁₄₄H₁₇₆N₄₀O₂₈S₈Si₈ (MW 3396.40) C 45.12, H 5.80, N 18.47; found C 45.16, H 5.88,
137 N 18.51%.

138 Synthesis of octavinylsilsesquioxane (**POSS-vinyl**): Formation of **POSS-vinyl** was realized based on
139 literature data.¹⁴ Thus, acid Amberlite of medium porosity (40 g) was washed with concentrated
140 hydrochloric acid, water and methanol before charging it into a 500 mL flask, which was equipped
141 with a magnetic stirrer. Methanol (150 mL) was added and stirred at 30°C. Vinyltrichlorosilane (4.0
142 mL, 0.04 mol) was added slowly with stirring to the Amberlite methanolic solution. The stirring
143 continued at room temperature for 10 h during which white microcrystals were deposited on the wall
144 of the flask. Methanol was decanted into a pre-prepared 500 mL flask (to be reused in the next
145 experiment). Dichloromethane was added to dissolve the microcrystals and the Amberlite was filtered
146 out for reuse in subsequent experiments. The solvent was evaporated and the vinyl-T8 microcrystals
147 washed several times with methanol.

148 ¹H NMR (CDCl₃) δ (ppm): 5.69–6.15 (m, H₂C=CH–, 24H); ¹³C NMR (CDCl₃) δ (ppm): 128.70 (C1),
149 136.95 (C2); ²⁹Si NMR (CDCl₃) δ (ppm): –79.8, –80.6 (–SiCH=CH₂).

150 Synthesis of **POSS-S-Cl**: **POSS-Vinyl** (2.0 g, 3.16 x 10⁻³ mol) was dissolved in anhydrous toluene
151 (15 mL) under N₂ atmosphere. The radical initiator AIBN (0.2 g, 1.22 x 10⁻³ mol) was added to **POSS-**
152 **Vinyl** solution and the reaction mixture was heated to 40 °C. Then the linker 3-chloropropanethiol
153 (2.64 mL, 27 x 10⁻³ mol) was slowly added to the mixture and the reaction was stirred for 13 h at
154 60°C. After cooling the reaction at room temperature, the supernatant was removed, and the gel was
155 solubilized in dichloromethane (5.0 mL) and precipitated with hexane (5 x 50 mL) at 0°C. Finally,

156 the gel was dried under reduced pressure to give the desired product as transparent viscous gel (1.97
157 g, yield 99%).

158 ^1H NMR (300 MHz, CDCl_3) δ (ppm): 1.08 (t, 16H, $-\text{SiCH}_2-$); 2.1 (m, 16H, $-\text{SCH}_2\text{CH}_2-$); 2.63
159 (overlapped, 16H, $-\text{SCH}_2-$); 2.65 (overlapped, 16H, $\text{SiCH}_2\text{CH}_2-\text{S}-$); 3.71 (t, 16H, $-\text{CH}_2\text{Cl}$). ^{13}C NMR
160 (100 MHz, CDCl_3) δ (ppm): 42.5, 32.6, 29.8, 26.3, 14.1. ^{29}Si NMR (99 MHz) δ (ppm): -68. Elemental
161 analysis (%) for $\text{C}_{40}\text{H}_{80}\text{Cl}_8\text{O}_{12}\text{S}_8\text{Si}_8$, calculated: C = 31.64, H = 5.30 S = 16.91; found: C = 31.89, H
162 = 5.28, S = 16.55.

163 Synthesis of **POSS-S-N₃**. **POSS-S-Cl** (1.5 g, 9.9×10^{-4} mol) and excess of NaN_3 (2.0 g) were added
164 to a flask equipped with a magnetic stirrer along with 15 mL of anhydrous *N,N*-dimethylformamide
165 (DMF). The reaction was carried out at 70°C for 2 days. After completion of the reaction, distilled
166 water was added, and the mixture was extracted with CH_2Cl_2 . Organic layers were dried over
167 anhydrous sodium carbonate, filtered, and concentrated under reduced pressure to obtain the desired
168 product as a yellow viscose liquid (1.23 g, Yield 82%)

169 ^1H NMR (300 MHz, CDCl_3) δ (ppm): 1.01 (t, 16H, $-\text{SiCH}_2-$); 1.90 (m, 16H, $-\text{SCH}_2\text{CH}_2-$); 2.58
170 (overlapped, 16H, $-\text{SCH}_2-$); 2.61 (overlapped, 16H, $\text{SiCH}_2\text{CH}_2-\text{S}-$); 3.60 (t, 16H, $-\text{CH}_2\text{Cl}$). ^{13}C NMR
171 (100 MHz, CDCl_3) δ (ppm): 41.9, 32.9, 28.8, 25.7, 13.6. ^{29}Si NMR (99 MHz) δ (ppm): -68. Elemental
172 analysis (%) for $\text{C}_{40}\text{H}_{80}\text{N}_{24}\text{O}_{12}\text{S}_8\text{Si}_8$, calculated: C = 30.59, H = 5.13, N = 21.41; found: C = 30.41, H
173 = 5.11, N = 21.44.

174 Synthesis of **POSS-S-D₈**: Under nitrogen atmosphere, *N*-dansyl propynyl, **D** (2.25 g, 7.8×10^{-3} mol)
175 was added to 10 mL THF/DMF (1:1) solution of **POSS-S-N₃** (1.23 g, 7.8×10^{-4} mol). CuBr (50%
176 mol equivalent) and PMDETA (50% mol equivalent) were successively added. The reaction mixture
177 was stirred at RT overnight. 0.02 M EDTA was added and extracted with DCM. Organic phase was
178 further washed with deionized water and Na_2SO_4 added. After filtration and concentration in a rotary
179 evaporator, the solid was recrystallized in chloroform/methanol (1:3) to give the desired product as a
180 light yellow solid (1.12 g, Yield 91%).

181 ¹H NMR (300 MHz, CDCl₃) δ (ppm): 1.09 (t, 16H, -SiCH₂-); 2.14 (m, 16H, -SCH₂CH₂-); 2.49 (t,
182 16H, -SCH₂-); 2.61 (t, 16H, SiCH₂CH₂-S-); 2.85 (s, 48H, Ar-N(CH₃)₂); 4.15 (t, 16H, -SCH₂CH₂CH₂-
183 N-); 4.30 (s, 16H, -CH₂NH); 7.1 (s, 8H, sulfonamide proton NH). ¹³C NMR (100 MHz, CDCl₃) δ
184 (ppm): 15.1, 25, 38, 45.1, 52, 53.3, 66.2, 116.0, 118.6, 121, 128.4, 135.8, 151. ²⁹Si NMR (99 MHz)
185 δ (ppm): - 67. FT-IR (cm⁻¹): ν(CH) 2966.6; (CN) 1678; (NCO) 1644.7 ν(C=C-Ar) 1741.9; ν(Si-O-
186 Si) 1161-1020; MS (API-ESI) m/z: 3875.98 [M+H]⁺; Elemental analysis (%) for
187 C₁₆₀H₂₀₈N₄₀O₂₈S₁₆Si₈; ; calculated: C = 48.56, H = 5.41 N = 13.98; found: C = 48.39, H = 5.52, N =
188 13.79.

189 *Photophysical characterization*

190 Absorption measurements: Steady state absorption spectra were recorded in a JASCO V-630
191 spectrophotometer. Quartz cells with 1 cm optical path length and 3 mL of capacity were employed.

192 Molar coefficient extinction, ε, was determined according to the Lambert-Beer law:

$$193 \text{ Abs} = C \cdot \epsilon \cdot L$$

194 Where, Abs is the absorbance of sample, C concentration, and L the optical path length of the cuvette.

195 Fluorescence experiments: Emission spectra were recorded on a JASCO FP-8500 spectrofluorometer
196 system, provided with a monochromator in the wavelength range of 200-850 nm. From the
197 intersection between normalized excitation and emission spectra the singlet energy was determined.

198 Fluorescence quantum yields were determined using 9,10-dimethylantracene as standard (0.95,
199 ETOH). Experiments were performed at 22 °C.

$$200 \phi_F = \frac{A_i}{A_{std}} \cdot \frac{Abs_{std}}{Abs_i} \cdot \frac{n}{n_{std}} \phi_{F(std)}$$

201 Where, A_i is the fluorescence area of the sample, A_{std} is the fluorescence area of standard, Abs and
202 Abs_{std} correspond to the absorbance intensity at excitation wavelength of the sample and standard,
203 respectively, and n is the refraction index of the solvent employed. Fluorescence lifetimes were
204 recorded on a PTI (Photon Technology International) fluorometer which includes a pulsed LED
205 excitation source, a sample holder, and a lifetime detector. For lifetime analysis, EasyLife X software

206 was used. The employed LEDs source was 340 nm. The excitation conditions are expressed in the
207 supplementary information.

208 *Photostability studies*

209 The two FLMs (**POSS-D₈** and **POSS-S-D₈**) and alkynyl dansyl precursor in THF, were irradiated
210 with a monochromatic light for 60 hours and photostability was monitored by absorption and
211 emission at interval of time. A conservative monochromatic light irradiation of the samples was
212 equally employed in our laboratory and the absorption profiles were monitored. For this, samples (1.0
213 x 10⁻⁵ M) were irradiated with Xenon arc lamp at irradiances of 0.039 W/cm² and 0.052 W/cm².

214 *Fingerprint development and imaging*

215 As far as this study is concerned, fingermarks were collected from 2 voluntary donors (27 years old
216 and 14 years old) and deposited on phone glassy surface. The donor rubbed his thumb on
217 forehead/nose tip and then it was press-stamped on selected substrate, immersed in FLM solution,
218 and rinsed with water or some organic solvents. The developed fingerprint in **POSS-D₈** or **POSS-S-**
219 **D₈** was illuminated with UV lamp (365 nm) and image taken with Samsung smartphone camera.

220

221 **3. Results and Discussion**

222 The 3D **POSS** nanohybrids were synthesized following a three-step procedure (Figure 1C). In the
223 case of **POSS-D₈**, catalytic treatment of 3-chloropropyltrimethoxysilane by di-*n*-butyltin dilaurate in
224 acidic methanol gave the desired octakis(3-chloropropyl)octasilsesquioxane (**POSS-Cl**). Then,
225 typical reaction of **POSS-Cl** with sodium azide in dimethylformamide afforded the corresponding
226 azide-substituted material octakis(3-azidopropyl)octasilsesquioxane (**POSS-N₃**). Last step involved
227 the copper “click” reaction between the resultant **POSS-N₃** and 5-(dimethylamino)-*N*-(2-propynyl)-
228 1-naphthalenesulfonamide (*N*-dansyl propynyl, **D**) which had been previously synthesized according
229 to literature.¹¹ Our desired product, **POSS-D₈**, was obtained in high yield (78%) as a light yellow
230 solid. Regarding **POSS-S-D₈**, the protocol commenced with the octavinylsilsesquioxane (**POSS-**

231 **Vinyl**) which was fabricated as described in the experimental section.¹⁴ Thus, treatment of **POSS-**
232 **Vinyl** with a radical initiator (azobisisobutyronitrile, AIBN) in the presence of 3-chloro-1-
233 propanethiol afforded quantitatively the octakis(2-((3-chloropropyl) thio)ethyl)octasilsesquioxane
234 (**POSS-S-Cl**). Following the same synthetic sequence as abovementioned, **POSS-S-Cl** was converted
235 into octakis(2-((3-azidopropyl)thio)ethyl)octasilsesquioxane (**POSS-S-N₃**) by azidation in high yield
236 (82%) and, subsequently formation of the final product, **POSS-S-D₈**, was obtained in excellent yield
237 (91%) by the CuBr/PMDETA catalyzed “click” reaction of **POSS-S-N₃** with *N*-dansyl propynyl **D**.
238 The chemical structures of **POSS-D₈** and **POSS-S-D₈** were fully characterized by NMR spectroscopy
239 (Figures S1-S6). For **POSS-D₈**, characteristic hydrogen resonances of -SiCH₂CH₂CH₂-N, dansyl-
240 N(CH₃)₂, downfield sulfonamide singlet proton (δ 7.15) and dansyl aromatic protons were clearly
241 identified. Additionally, the presence of the triazole singlet proton (δ 7.7) evidenced that the “click”
242 reaction was succeeded. Furthermore, ²⁹Si NMR spectrum of **POSS-D₈** (Figure S7) showed a strong
243 single peak, confirming that the Si–O–Si skeleton was not affected during the different synthetic
244 steps. As a matter of fact, FTIR spectra reflected this fact where the structural evolution **POSS-Cl** →
245 **POSS-N₃** → **POSS-D₈** was displayed (Figure S8). To highlight the disappearance of the azide group
246 after the “click” reaction together with the appearance of carbon-carbon double bond which
247 corresponded to the aromatic dansyl chromophore anchored to the Si–O–Si skeleton. In the case of
248 **POSS-S-D₈**, protons due to -SiCH₂CH₂-S-(CH₂)₃- arms of **POSS**, sulfonamide, triazole, -N(CH₃)₂,
249 -CH₂NH- and dansyl aromatics were clearly assigned in the ¹H NMR spectrum, confirming the
250 chemical structure (Figures S9-S10). Again, the integrity of the nanocage was confirmed by the
251 presence of one signal in the ²⁹Si NMR spectrum (Figure S11), which is typical of T8R8 structure
252 corresponding to the T3 silicon units.^{15,16} Finally, on the basis of the FTIR spectra (Figure S12),
253 structural evolution **POSS-S-Cl** → **POSS-S-N₃** → **POSS-S-D₈** was also observed. Energy-
254 minimized structure of nanohybrids **POSS-D₈** and **POSS-S-D₈** showed a molecular dimension of ca.

255 3.2 nm and 4 nm, respectively (Figure S13). Optical properties of **POSS-D₈** and **POSS-S-D₈** were
 256 detailed studied in several solvents (Figure 1D and Table 1).

257

Table 1. Photophysical properties of **POSS-D₈** and **POSS-S-D₈**

solvent	POSS-D₈							POSS-S-D₈						
	^a $\lambda_{\text{abs,max}}$	^a $\lambda_{\text{em,max}}$	^b ϵ	^c Stokes	^d E _S	ϕ_{F}	ϕ_{nrad}	^a $\lambda_{\text{abs,max}}$	^a $\lambda_{\text{em,max}}$	^b ϵ	^c Stokes	^d E _S	ϕ_{F}	ϕ_{nrad}
DMF	338	519	54510	10328	67.4	0.33	0.67	335	519	2998	10582	67.3	0.91	0.09
ACN	338	522	40350	10429	66.5	0.31	0.69	339	522	2456	10341	66.6	0.64	0.26
THF	341	506	62019	9562	70.2	0.50	0.50	340	509	5469	9765	68.5	0.70	0.30
DCM	341	512	57848	9794	67.0	0.46	0.54	340	514	3675	9956	66.9	1	0

^ain nm; ^bin M⁻¹cm⁻¹; ^cin cm⁻¹; ^din kcal mol⁻¹

258

259 Similar absorption spectra of both nanohybrids were found in which the absorption band at UVA
 260 region was clearly dominated by the dansyl-type chromophore (Figures S14-S15). They presented
 261 very high values of Stoke's shifts as typically found for dansylated derivatives.¹⁷ The most important
 262 difference was attributed to the corresponding molar absorption coefficients (ϵ), being remarkably
 263 higher in the case of **POSS-D₈** than those for **POSS-S-D₈**. On the contrary, fluorescence quantum
 264 yields (ϕ_{F}) **POSS-S-D₈** were found to be in general 2 times higher than the values observed for
 265 nanohybrid **POSS-D₈**, with the occurrence that the sulfur bridge may influence in the radiative and
 266 non-radiative pathways of the material. As a general trend, higher values of ϕ_{F} were detected in
 267 moderately polar solvents. To noteworthy that the ϕ_{F} of **POSS-S-D₈** was found to be the unity in
 268 DCM, indicating no energetic losses. A satisfactory fitting was obtained by considering a
 269 biexponential function for the emission decay traces of **POSS-D₈** and **POSS-S-D₈** (Table 2 and
 270 Figures S16-S17). This was in fully agreement with previously reported data⁸ for similar **POSS**
 271 nanohybrid containing only one dansyl chromophore. Thus, an intramolecular charge transfer (ICT)
 272 state (shorter lifetimes) and possible aggregates (longer lifetimes) could be the responsible of these
 273 two emissive lifetimes. However, contribution of the longer lifetime component was actually in the
 274 same extend or even higher, especially in moderately polar solvents, indicating unambiguously

275 formation of aggregates. As a premise, it could evidence for enhancing the fluorescence quantum
276 yield and stability of the nanohybrids.

277

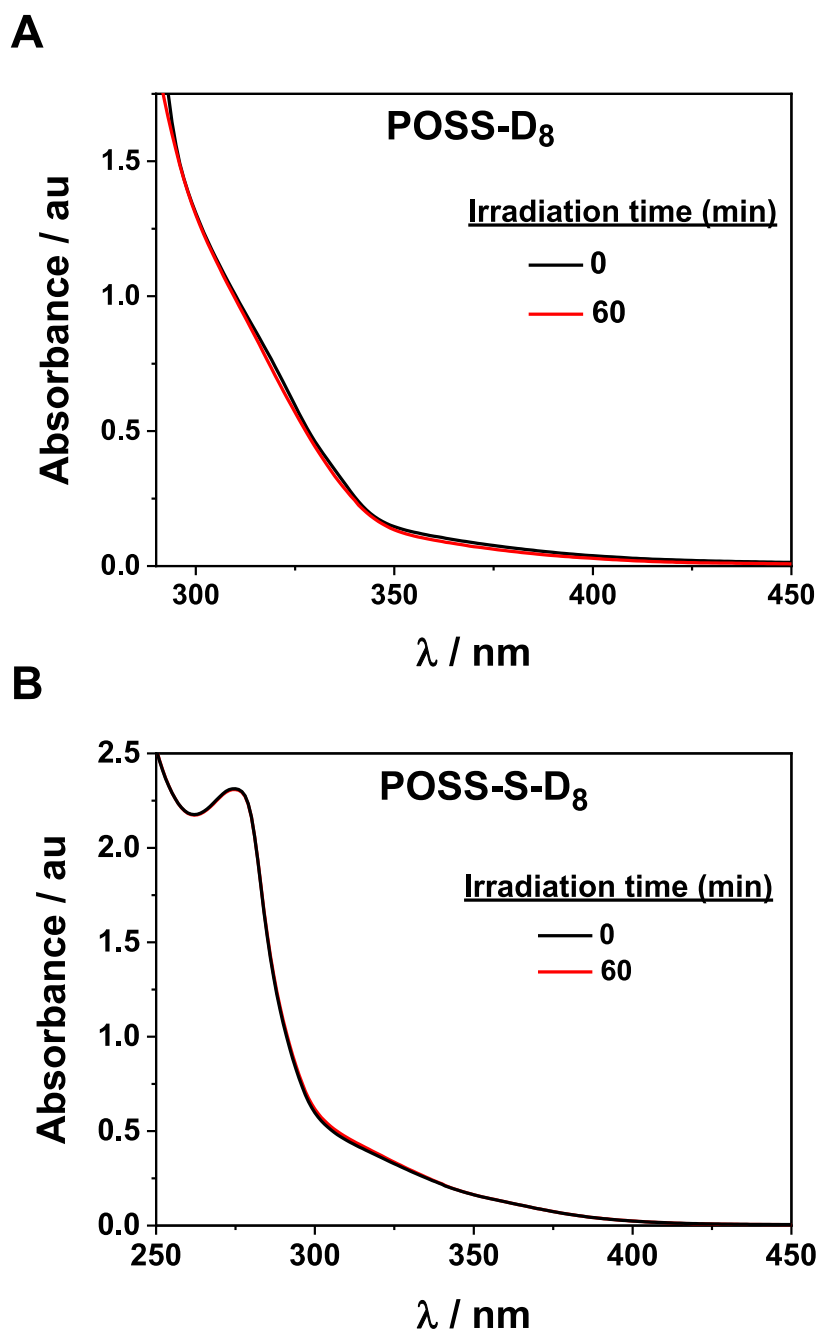
Table 2. Fluorescence lifetimes^a of **POSS-D₈** and **POSS-S-D₈**

solvent	POSS-D ₈	POSS-S-D ₈
	τ_F (τ_1 ; τ_2)	τ_F (τ_1 ; τ_2)
DMF	11.7 (53%); 25.4 (47%)	13.1 (62%); 31.1 (38%)
ACN	11.7 (77%); 27.5 (23%)	13.2 (81%); 36.6 (19%)
THF	10.1 (53%); 23.8 (47%)	11.1 (60%); 29.4 (40%)
DCM	11.6 (40%); 26.2 (60%)	12.3 (48%); 29.8 (52%)

^ain ns; in brackets the contribution of each lifetime.

278

279 Photostability of **POSS-D₈** and **POSS-S-D₈** was evaluated by monitoring their absorption spectra
280 before and after (60 min) monochromatic light irradiation ($\lambda_{irr} = 340$ nm) in THF as solvent (Figure
281 2). Hence, the absorption spectra of both materials were completely similar even after 60 min of
282 continuous photolysis, showing a magnificent photostable properties. In order to use more sensitive
283 analytical technique, emission spectra were also recorded before and after irradiation (Figure S18).
284 Here, **POSS-D₈** and **POSS-S-D₈** retained the 90% and 86%, respectively, of the fluorescence
285 intensity.



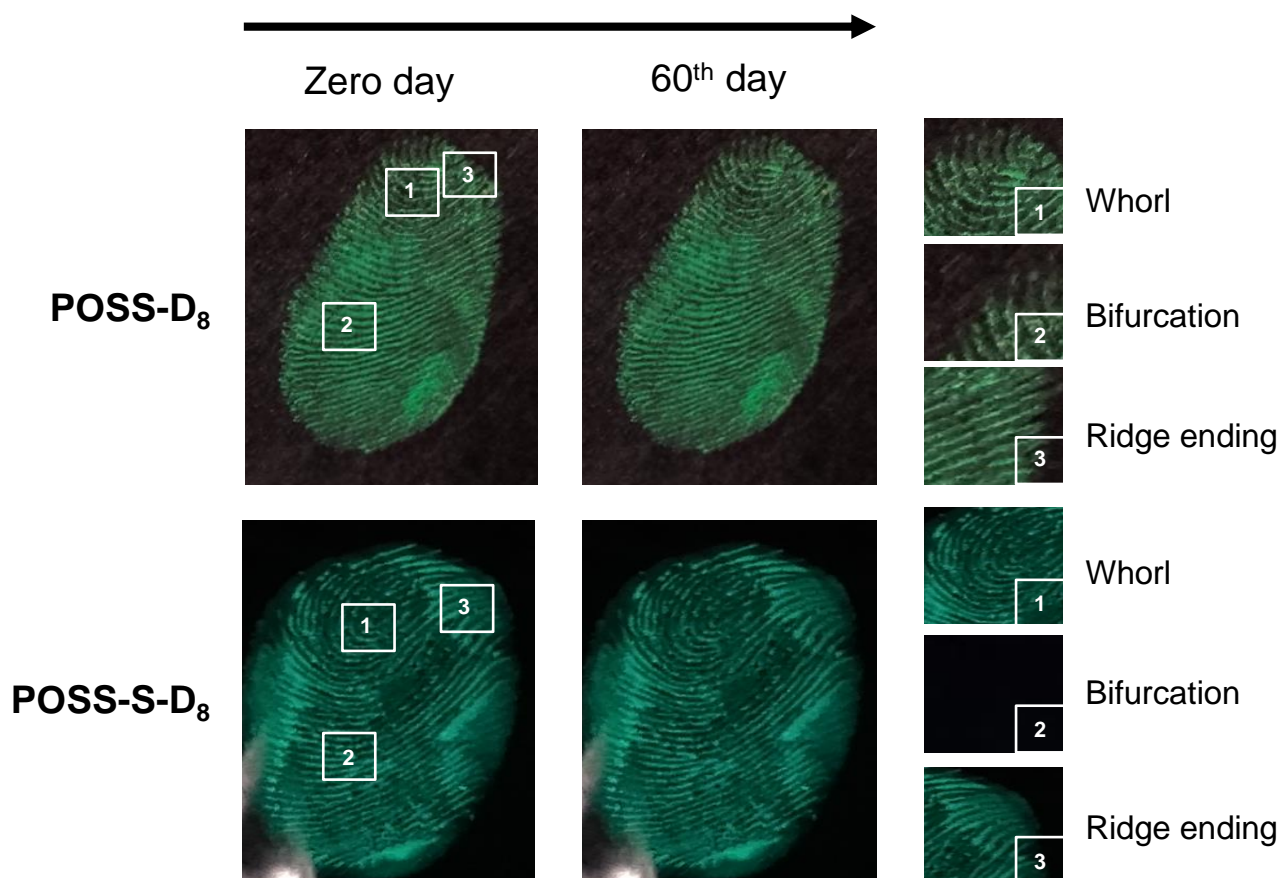
286

287 **Figure 2.** Absorption spectra of **A) POSS-D₈** (0.004 mM) and **B) POSS-S-D₈** (0.04 mM) in aerated
 288 THF before and after monochromatic light irradiation ($\lambda_{\text{irr}} = 340$ nm).

289

290 A judicious balance of hydrophobic and π - π interactions have been recognized in previous reports for
 291 the application of FLMs in LF detection.^{8,9,10} Accordingly, our FLMs were designed based on the
 292 combination of a Si-O-Si skeleton and multiple dansyl scaffolds. Figure 3 shows images

293 corresponding to fresh (0 day) and aged fingerprints (i.e. stored at RT for 60 days) (see ESI for
294 details). While undeveloped fingerprint patterns were hardly visible under UV (365 nm) or visible
295 light, those developed under diluted solution of **POSS-D₈** or **POSS-S-D₈** apparently exhibited
296 enhanced legibility due to greater contrast between the fluorescent ridge and non-fluorescent furrow.
297 Importantly, the brightness, contrast and general visual legibility remained intact for at least 60 days,
298 indicating a very good photostability of both FLMs. This is ascribed to the structural hydrophobic
299 features of the nanohybrids, which provide an optimal affinity to the amino acid-based oily
300 compounds present in the fingerprints through hydrogen bonding (e.g. S=O××××H-N (amino
301 acid)).^{18,19} Moreover, enlarged areas showed whorl, bifurcation, and ridge ending (Figure 3, right
302 side), which fulfill the requirements for fingerprint identification.
303



304
305 **Figure 3.** Representative digital photos of fingerprints on smooth phone-glass surfaces detected by
306 means of **POSS-D₈** and **POSS-S-D₈**. Enlarged zones identified with numbers are given on the right.

307 **4. Conclusions**

308 In summary, two novel octa-dansyl fluorescently labeled POSS (POSS-D8 and POSS-S-D8) have
309 been easily synthesized via “click” chemistry. These nanohybrids were fully characterized and the
310 photophysical study revealed significantly higher molar absorption coefficient for POSS-D8, while
311 the fluorescence quantum yield was 2 times higher in the case of POSS-S-D8. Both FLMs displayed
312 exceptionally distinguished photostability well above that of the N-dansyl propynyl precursor. The
313 two photoresponsive octadansyl labeled POSS enabled the detection of latent fingerprints on phone
314 glassy surfaces with very good legibility according to the requirements for forensic applications.

315

316 **Declaration of competing interest**

317 The authors declare that they have no known competing financial interests or personal relationships
318 that could have appeared to influence the work reported in this paper.

319

320 **Acknowledgment**

321 Financial support by the Alexander von Humboldt Foundation (Georg Forster Research Fellowship
322 to E.O. Dare), Generalitat Valenciana (CIDEAGENT/2018/044) and Universität Regensburg is
323 gratefully acknowledged. Laboratory assistance from MSc A. Abramov and Dr. B. Maiti (Universität
324 Regensburg) is deeply acknowledged. D.D.D. thanks the DFG for the Heisenberg Professorship
325 Award and the Spanish Ministry of Science, Innovation and Universities for the Senior Beatriz
326 Galindo Award (Distinguished Researcher; BEAGAL18/00166).

327

328 **Appendix A. Supplementary data**

329 Supplementary data to this article can be found online at

330

331

-
- ¹ Y. Liu, F. Han, F. Li, Y. Zhao, M. Chen, Z. Xu, X. Zheng, H. Hu, J. Yao, T. Guo, W. Lin, Y. Zheng, B. You, P. Liu, Y. Li and L. Qian. Inkjet-printed unclonable quantum dot fluorescent anticounterfeiting labels with artificial intelligence authentication. *Nat. Commun.* 2019, **10**, 2409.
- ² K.-K. Liu, C.-X. Shan, G.-H. He, R.-Q. Wang, Z.-P. Sun, Q. Liu, L. Dong and D.-Z. Shen. Advanced encryption based on fluorescence quenching of ZnO nanoparticles *J. Mater. Chem. C* 2017, **5**, 7167.
- ³ K. Partha, B. Subrata, P. Prafull, S. T. Chandra and K. Pathik. Tailoring of structural and photoluminescence emissions by Mn and Cu co-doping in 2D nanostructures of ZnS for the visualization of latent fingerprints and generation of white light. *Nanoscale* 2019, **11**, 2017.
- ⁴ M. Wang, M. Li, A. Yu, Y. Zhu, M. Yang and C. Mao. Fluorescent nanomaterials for the development of latent fingerprints in forensic sciences. *Adv. Funct Mater.* 2017, **27**, 1606243, and references therein.
- ⁵ F. K. Kanodarwala, S. Moret, X. Spindler, C. Lennard and C. Roux. Nanoparticles used for fingerprint detection—A comprehensive review. *WIREs Forensic Sci.* 2019, **1**, e1341, and references therein.
- ⁶ P. Wu, C. Xu, X. Hou, J.-J. Xu and H.-Y. Chen. Dual-emitting quantum dot nanohybrid for imaging of latent fingerprints: simultaneous identification of individuals and traffic light-type visualization of TNT. *Chem. Sci.* 2015, **6**, 4445.
- ⁷ F. Li, H. Li and T. Cui. One-step synthesis of solid state luminescent carbon-based silica nanohybrids for imaging of latent fingerprints. *Opt. Mater.* 2017, **73**, 459.
- ⁸ E. O. Dare, V. Vendrell-Criado, M. C. Jiménez, R. Pérez-Ruiz and D. Díaz Díaz. Novel Fluorescent Labeled Octasilsesquioxanes Nanohybrids as Potential Materials for Latent Fingerprinting Detection. *Chem. J. Eur.* 2020, doi: [10.1002/chem.202001908](https://doi.org/10.1002/chem.202001908).

-
- ⁹ R. L. Ma, Y. Zhao, F. Gao and K. Han. Future direction of latent fingerprints development techniques. *Chin. J. Forensic Sci.* 2016, **2**, 64.
- ¹⁰ J. B. Friesen. Forensic Chemistry: The revelation of latent fingerprints. *J. Chem. Educ.* 2015, **92**, 497.
- ¹¹ B. Fabrizio, F. Daniele, L. Marco, P. Luca, T. Claudio Z. Nelsi. Synthesis and Photophysical Properties of Fluorescent Derivatives of Methylmercury. *Organometallics* 1996, **15**, 2415.
- ¹² M. Bogdan, D. Michal, M. Hieronim, K. Maciej. New, Effective Method of Synthesis and Structural Characterization of Octakis(3-chloropropyl)octasilsesquioxane. *Organometallics* 2008, **27**, 793.
- ¹³ W. Yuan, X. Liu, H. Zou, J. Ren. Environment-induced nanostructural dynamical-change based on supramolecular self-assembly of cyclodextrin and star-shaped poly(ethylene oxide) with polyhedral oligomeric silsesquioxane core. *Polymer* 2013, **54**, 5374.
- ¹⁴ E. O. Dare, L.-K. Li, J. Peng. Modified procedure for improved synthesis of some octameric silsesquioxanes via hydrolytic polycondensation in the presence of Amberlite ion-exchange resins. *Dalton Trans.* 2006, 3668.
- ¹⁵ M. E. Pérez-Ojeda, B. Trastoy, A. Rol, M. D. Chiara, I. Garcia-Moreno and J. L. Chiara. Controlled click-assembly of well-defined hetero-bifunctional cubic silsesquioxanes and their application in targeted bioimaging. *Chem. Eur. J.* 2013, **19**, 6630.
- ¹⁶ B. J. Hendan and H. C. Marsmann. Semipräparative rennung gemischt substituierter Octa-(organylsilsesquioxane) mittels Normal-Phase-HPLC und ihre ²⁹Si-NMR-spektroskopische Unters. *J. Organomet. Chem.* 1994, **483**, 33.
- ¹⁷ M. Montalti, L. Prodi, N. Zaccheroni, G. Battistini, S. Marcus, F. Mancin, E. Rampazzo and V. Tonellato. Size effect on the fluorescence properties of dansyl-doped silica nanoparticles. *Langmuir* 2006, **22**, 5877.

¹⁸ C. Hong, L. M. Rong, C. Yun and J. F. Li. Fluorescence Development of Latent Fingerprint with Conjugated Polymer Nanoparticles in Aqueous Colloidal Solution. *ACS Appl. Mater. Interfaces* 2017, **9**, 4908.

¹⁹ H. Chen, K. Chang, X. Men, K. Sun, X. Fang, C. Ma, Y. Zhao, S. Yin, W. Qin and C. Wu. Covalent Patterning and Rapid Visualization of Latent Fingerprints with Photo-Cross-Linkable Semiconductor Polymer Dots *ACS Appl. Mater. Interfaces* 2015, **7**, 14477.